

# Accuracy Considerations in Microstrip Surface Impedance Measurements

Juan M.O'Callaghan, Carles Sans, Carlos Collado, Eduard Canet, Rafael Pous.  
 Universitat Politecnica de Catalunya. Campus Nord-D3. Barcelona 08034, Spain.

Josep Fontcuberta.  
 ICMAB-CSIC. Campus UAB. Bellaterra 08193, Spain.

**Abstract**— An approach is proposed for the design, measurement and data extraction of superconducting microstrip resonators used in determination of surface resistance and penetration depth. Major sources of error are analyzed and procedures to minimize them are given.

## I. INTRODUCTION

Measurement of microstrip ring resonators has been proven to be a useful technique for characterizing surface impedance of superconducting thin films [1] (or equivalently, their surface resistance  $R_s$  and penetration depth  $\lambda_L$ ). However, there are still parameters that can be optimized in their design and features of their structure (like low-loss coupling) that can be further exploited to facilitate their measurement. In this paper we analyze the tradeoffs between accuracy and dynamic range; modify Aitken's algorithm [2] for the particular case of cryogenic 1-port resonator measurements; and present a simple method to predict the uncertainty in  $R_s$  due to tolerances in the loss tangent of the dielectric substrate.

## II. BASICS

The basic structure of a microstrip ring resonator (Fig. 1) consists of an access line, a coupling gap and the microstrip ring itself. From its symmetry, it can be argued that the current in the ring, at the point diametrically opposed to the coupling gap, must be zero. Cutting the ring at that point would not alter its electric properties and therefore, its impedance seen from the coupling gap has to be equal to that of two parallel, open-ended stubs whose length would be half the perimeter of the ring (Fig. 1). From this equivalent circuit, it is apparent that there are parallel resonances when the perimeter of the ring is a multiple of the wavelength. The lumped equivalent circuit of the ring can thus be assumed to be like that shown in Fig. 2, in which the values of  $L_{ring}$ ,  $C$  and  $R_{ring}$  are related to the parameters of the ring line [3]:

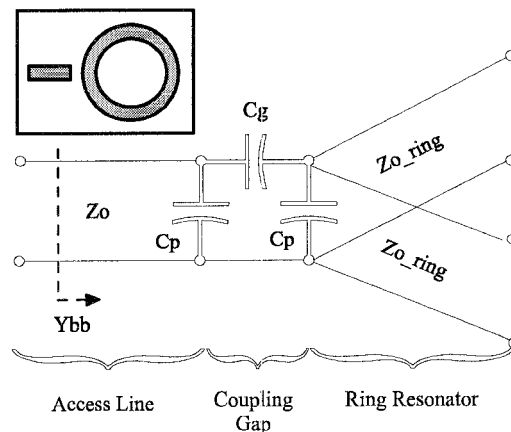


Fig. 1. Layout of microstrip resonator (inset) and distributed equivalent circuit.  $Z_o$  and  $Z_{o\_ring}$  are the characteristic impedances of the access line and ring line, respectively. The effect of the gap is modeled by two shunt capacitances ( $C_p$ ) and a through capacitance ( $C_g$ ) [4].

$$L_{ring} = \frac{Z_{o\_ring}}{n\pi\omega_o}; C = C_p + \frac{n\pi}{Z_{o\_ring}\omega_o}; \quad (1)$$

$$R_{ring} = \frac{Z_{o\_ring}}{\alpha 2\pi r_{av}}; \omega_o = \frac{1}{\sqrt{L_{ring}C}}$$

where  $r_{av}$  is the average radius of the microstrip ring,  $\alpha$  its attenuation coefficient, and  $n$  the order of the resonance. The remaining variables in (1) are described in Fig. 1.

The shunt combination of  $L_{ring}$ ,  $C$  and  $R_{ring}$  (Fig. 2) produces an admittance  $Y$  which can be approximated by

$$Y \approx \frac{1}{R_{ring}} [1 + j2Q_o\delta]; \quad \delta = \frac{\omega - \omega_o}{\omega_o}, \quad (2)$$

where  $\delta$  is a normalized frequency variable and  $Q_o$  is the unloaded quality factor:

$$Q_o = \frac{R_{ring}}{\omega_o L_{ring}}. \quad (3)$$

The combined effect of the gap reactance and a proper selection of reference plane (the "detuned short plane" in Figs.

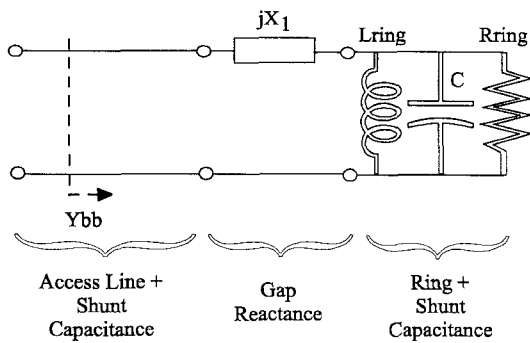


Fig. 2. Lumped equivalent circuit of a microstrip resonator. The shunt capacitances  $C_p$  are absorbed in the tank circuit and as an additional length of the access line.

1 and 2 [5]) can be shown to be equivalent to a sort of impedance transformation by which, instead of  $Y$ , the admittance to be measured is:

$$Y_{bb} \approx \frac{1}{Z_o \beta} \left[ 1 + j2Q_o(\delta - \delta_o) \right]; \delta_o = \frac{\beta X_1}{2Q_o Z_o} \quad (4)$$

where  $\beta$  is the coupling coefficient:

$$\beta = \frac{R_{ring}/Z_o}{1 + (X_1/Z_o)^2}; \quad X_1 = \frac{-1}{\omega_o C_g} \quad (5)$$

A secondary effect of the gap reactance—besides the admittance scaling implicit in (2) and (4)—is to shift the resonant frequency of  $Y_{bb}$  with respect that of  $Y$ : instead of resonating at  $\omega = \omega_o$  (or  $\delta = 0$ ),  $Y_{bb}$  becomes real at the frequency that makes  $\delta = \delta_o$ .

Finally, the experimental procedure to be used (Sect. 5 of [2]) obtains the unloaded quality factor ( $Q_o$ ) and resonant frequency  $f_o = \omega_o/(2\pi)$  from measurements of the magnitude of the reflection coefficient produced by  $Y_{bb}$ . Since these measurements are independent of the reference plane, the exact location of the detuned short plane in the access line does not need to be known.

### III. DETERMINATION OF $Q_o, f_o$

Previous work on determination of quality factors [2, 6] is based on the assumption that distributed losses in the lines accessing the resonator can be accurately accounted for and they concentrate on other, lumped-type losses that may be present in the structure coupling the signal into the resonating structure. To account for distributed losses, one has to be able to replace the resonator by a short standard, while keeping the measurement setup unchanged.

This is not the case in a cryogenic system where, usually, a calibration at room temperature is done and then the

resonator is connected and the system is cooled down. The characteristics of the measurement setup do not remain completely invariant during calibration and measurement. Of them, the most influential on measurement results is the change in the access line loss. On the other hand, the coupling mechanism is virtually lossless, so the corrections suggested in [2,6] are not necessary in our case.

In an ideal setup, all what is needed to resolve the uncertainty in the access line loss is to observe the magnitude of the reflection coefficient away from resonance and adjust the reference level to make it unity (0 dB). In practice, problems may arise from imperfect calibrations, which introduce a small ripple in the frequency dependence of this reflection coefficient. An alternative approach, which is more robust to imperfect calibrations, is to scale the measured reflection coefficients by finding the multiplicative constant that makes the resonance circle tangent to the edge of the Smith chart. Previous to that scaling, it is useful to reject all data points (frequency-reflection coefficient pairs) not belonging to the resonance circle and perform a least squares, non iterative fit of a circle (Appendix I). Besides reducing sensitivity to experimental errors, this step also reduces the number of points to be handled, which facilitates automated data acquisition and processing. Once the scaling is done, the scalar version of Aitken's procedure [2], with lossless coupling is applied to find  $Q_o$ , the coupling coefficient  $\beta$ , and the loaded resonant frequency  $f'$  (the one for which  $Y_{bb}$  is real).

Another possible improvement on that procedure is a better estimation of the unloaded resonant frequency  $f_o$ , which in [2] is assumed to be equal to  $f'$ . This can be done by recognizing that  $\delta = \delta_o$  for  $f = f'$ :

$$f_o = f' - \Delta f \frac{\beta X_1}{2Z_o} \quad (6)$$

where  $Q_o = f_o/\Delta f$  being  $\Delta f$  the bandwidth between the two frequency points for which  $\rho_{bb}$  (the magnitude of the reflection coefficient corresponding to  $Y_{bb}$ ) satisfies [2]:

$$\rho_{bb}^2 = \frac{(1 - \beta)^2 + 1}{(1 + \beta)^2 + 1} \quad (7)$$

### IV. EXTRACTION OF $R_s$ AND $\lambda_L$

Once accurate values are obtained for  $Q_o, f_o$ , they have to be related to the parameters that characterize the properties of the superconducting material: typically its surface resistance  $R_s$  and penetration depth  $\lambda_L$ . This is done (as in [1]) by relating the internal impedance per unit length (which depends on the material and the geometry of the line) to the surface impedance of the material. This results in a surface resistance  $R_s$  that depends on the quality factor

$Q_o$  and a penetration depth  $\lambda_L$  that can be determined from the temperature dependence of the resonant frequency  $f_o$ .

As an extension of the extraction procedure outlined in [1], one can easily calculate the uncertainty in surface resistance due to an uncertainty in the loss tangent of the dielectric, since the total loss is a linear combination of both [1,4]:

$$Q_o = \frac{n}{2r_{av}\alpha}; \quad \alpha = C_1R_s + C_2\tan\delta. \quad (8)$$

Based on the second equation in (8), our software can display a "loss uncertainty line", from which a range of possible surface resistances can be predicted from the measurements and the specifications of the dielectric substrate.

## V. DESIGN GUIDELINES

There are only three parameters that need special considerations when designing the layout of a microstrip resonator: gap size, width of the microstrip in the ring and average ring radius. The most critical of them is the coupling gap size, since it plays an important role in the accuracy of  $R_s$  and its range of measurable values.

Adjustment of the gap size in the layout causes a change in the series reactance  $X_1$  and can be used to adjust the coupling coefficient  $\beta$ . However,  $\beta$  also depends on losses in the ring, which make it increase sharply when the resonator undergoes a normal to superconducting transition (see (1) and (5)). Furthermore, the value of  $\beta$  has a significant effect on the accuracy with which the unloaded quality factor  $Q_o$  can be extracted. An extension of the analysis in [2] (Appendix II) shows that the maximum relative error in  $Q_o$  follows the dependence with  $\beta$  shown in Fig. 3. For a system with a measurement uncertainty of  $\pm 0.05$  dB in mag-

nitude of reflection coefficient and a maximum acceptable error of 10% in  $Q_o$ , there is a 60:1 ratio between the maximum and minimum acceptable values of  $\beta$ . This range is much smaller than the variation occurring in  $\beta$  when the material undergoes the transition to a superconducting state and –since surface resistance is ultimately extracted from  $Q_o$ – it limits the range of  $R_s$  that can be measured with a given resonator. Thus, it is desirable to adjust the coupling gap so that the upper acceptable value of  $\beta$  will be obtained with the lowest attenuation constant  $\alpha$  that is anticipated.

The determination of the two remaining parameters is not as critical: the average ring radius  $r_{av}$  has to be made as large as possible, without getting too close to the edges of the film where the superconductive material might be degraded; and the width of the microstrip in the ring  $w$  has to be much smaller than the average radius while being within the range of validity of microstrip design equations [4].

## VI. CONCLUSION

The main factors affecting accuracy in the determination of  $R_s$  and  $\lambda_L$  through measurement of microstrip resonators have been analyzed. The design of the coupling gap and its effects on the errors in the unloaded quality factor has been quantified. Enhanced accuracy can be obtained by proper design of the gap, a least-squares fitting of the resonance circle, compensation of access line loss, and a correction of the effect of the coupling reactance in the resonance frequency. Total measured losses, surface resistance and dielectric loss tangent are related through the equation of a line, which allows an easy estimation of upper bounds in  $R_s$  or its uncertainty due to tolerances in loss tangent.

## APPENDIX I-LEAST SQUARES FIT OF A CIRCLE

The problem of fitting a circle to a set of experimental reflection coefficients can be formulated in terms of an overdetermined system of equations that can be adjusted through a pseudoinverse [7] (Fig. AI.1). If there are  $n$  different values of reflection coefficient  $\Gamma_j; j = 1 \dots n$ , this overdetermined system is:

$$\mathbf{A} \mathbf{z} \approx \mathbf{b} \quad (\text{AI-1})$$

with

$$\mathbf{A} = \begin{pmatrix} \text{Re}(\Gamma_1) & \text{Im}(\Gamma_1) & 1 \\ \text{Re}(\Gamma_2) & \text{Im}(\Gamma_2) & 1 \\ \vdots & \vdots & \vdots \\ \text{Re}(\Gamma_n) & \text{Im}(\Gamma_n) & 1 \end{pmatrix}; \quad \mathbf{z} = \begin{pmatrix} c_1 \\ c_2 \\ c_3 \end{pmatrix}; \quad \mathbf{b} = \begin{pmatrix} -|\Gamma_1|^2 \\ -|\Gamma_2|^2 \\ \vdots \\ -|\Gamma_n|^2 \end{pmatrix} \quad (\text{AI-2})$$

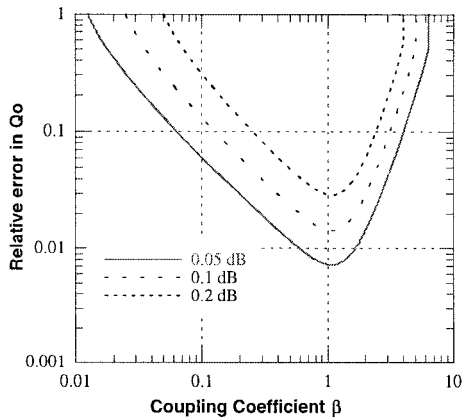


Fig.3. Maximum relative error in  $Q_o$  as a function of input coupling coefficient, for three different values of uncertainty in the measurement of reflection coefficient magnitude ( $\pm 0.05$ ,  $\pm 0.1$ ,  $\pm 0.2$  dB).

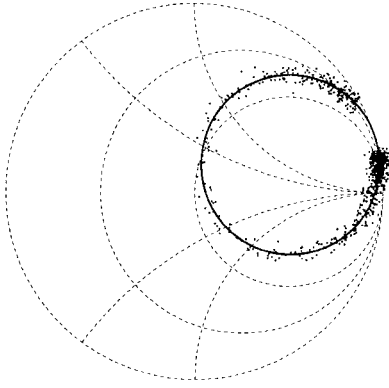


Fig. A1.1. Example of non-iterative least squares fit of a resonance circle ( $Q_o=1000$ ,  $\beta=0.9$ ) on simulated data points. Noise is exaggerated for illustration purposes.

where the values of  $c_1, c_2, c_3$  have to be found to minimize the error between  $\mathbf{A}\mathbf{z}$  and  $\mathbf{b}$ . This can be done either by solving the system of normal equations:

$$\mathbf{A}^T \mathbf{A} \mathbf{z} = \mathbf{A}^T \mathbf{b} \quad (\text{AI-3})$$

or using a pseudoinverse subroutine, common in most mathematical software. Once  $c_1, c_2, c_3$  are known, the radius  $R$  and coordinates of the center  $(x_o, y_o)$  can be found through the following equations:

$$x_o = -\frac{c_1}{2}; y_o = -\frac{c_2}{2}; R = \sqrt{\frac{1}{4}(c_1^2 + c_2^2) - c_3}. \quad (\text{AI-4})$$

#### APPENDIX II-RELATIVE ERRORS IN $Q_o$

The procedure for determining  $Q_o$  [2] is based on the dependence of the magnitude of the reflection coefficient in the access line ( $\rho_{bb}$ ) with  $\beta, Q_o, \delta$  and  $\delta_o$ :

$$\rho_{bb}^2 = \frac{(1-\beta)^2 + (2Q_o\delta')^2}{(1+\beta)^2 + (2Q_o\delta')^2} \quad (\text{AII-1})$$

where  $\delta' = \delta - \delta_o$ . The reflection coefficient magnitude  $\rho_{bb}$  is measured at the minimum of its frequency response,  $\rho_{min}$  (for which  $\delta' = 0$ ) and at two other points for which  $|2Q_o\delta'| = 1$  ( $\rho_{bb}$  is denoted as  $\rho_o$  in this particular case). The measurement of  $\rho_{min}$  is used to determine  $\beta$  and the band-

width at which  $\rho_{bb} = \rho_o$  determines  $Q_o$ . From (AII-1), the errors in  $2Q_o\delta'$  due to measurement errors in  $\rho_o$  and  $\rho_{min}$  can be found:

$$\left[1 + \Delta(2Q_o\delta')\right]^2 = 2(\beta + \Delta\beta) \frac{1 + (\rho_o + \Delta\rho_o)^2}{1 - (\rho_o + \Delta\rho_o)^2} - (\beta + \Delta\beta)^2 - 1 \quad (\text{AII-2})$$

where  $\Delta\beta$  is caused by errors in  $\rho_{min}$ .

Furthermore, since errors in frequency measurement are small,  $\delta'$  can be assumed to be errorless, which makes:

$$\Delta(2Q_o\delta') \approx 2\delta' \Delta Q_o = 2\delta' Q_o \frac{\Delta Q_o}{Q_o} \approx \frac{\Delta Q_o}{Q_o} \quad (\text{AII-3})$$

The relative error in  $Q_o$  shown in Fig. 3 has been estimated by numerical perturbation of  $\rho_o$  and  $\rho_{min}$  with a simple spreadsheet calculation involving (AII-1)-(AII-3) with  $\beta$  as a variable and the uncertainty in measurement of  $\rho_{bb}$  as a parameter.

#### ACKNOWLEDGMENTS

The authors are thankful to J. Santiso while at the Interdisciplinary Research Centre in Superconductivity for supplying YBCO films.

#### REFERENCES

- [1] C.M.Chorey, K.S. Kong, K.B. Basin, J.D. Warner, and T. Itoh, "YBCO superconducting ring resonators at millimeter-wave frequencies" IEEE Trans. on Microwave Theory and Tech., vol. 39 pp. 1480-1487, Sept. 1991.
- [2] J.E. Aitken, "Swept-frequency microwave Q-factor measurement" Proc. IEE, vol. 123, No. 9, pp.855-861 Sept. 1976.
- [3] G.L. Matthaei, *Microwave Filters, Impedance-Matching Networks and Coupling Structures*, McGraw-Hill, 1964.
- [4] Gupta K.C. *Microstrip Lines and Slotlines*, Artech House, 1979.
- [5] E.L. Ginzton, *Microwave Measurements*, McGraw-Hill, 1957.
- [6] D. Kajfez "Linear fractional curve fitting for measurement of high Q factors" IEEE Trans. on Microwave Theory and Tech., vol. 42 pp. 1149-1153, July 1994.
- [7] Steward. *Introduction to Matrix Computations*. Academic Press, 1973.